Bulk Assembly of Zero-Dimensional Organic Lead Bromide Hybrid with Efficient Blue Emission

Haoran Lin,[†] Chenkun Zhou,[‡] Maya Chaaban,[†] Liang-Jin Xu,[†] Yan Zhou,[†] Jennifer Neu,[§] Michael Worku,[#] Ella Berkwits,[†] Qingquan He,[†] Sujin Lee,[†] Xinsong Lin,[†] Theo Siegrist,[‡,§] Mao-Hua Du,[$] Biwu Ma*,[†,‡,#]

[†]Department of Chemistry and Biochemistry, Florida State University, Tallahassee, Florida 32306, United States

[‡]Department of Chemical and Biomedical Engineering, FAMU-FSU College of Engineering, Tallahassee, Florida 32310, United States

[§]National High Magnetic Field Laboratory, Florida State University, Tallahassee, Florida 32310, United States

[#]Materials Science and Engineering Program, Florida State University, Tallahassee, Florida 32306, United States

[$]Materials Science & Technology Division, Oak Ridge National Laboratory, Oak Ridge, Tennessee 37831, United States

ABSTRACT: Zero-dimensional (0D) organic metal halide hybrids are an emerging class of light emitting materials with exceptional photoluminescence quantum efficiencies (PLQEs), thanks to their perfect "host-guest" structures with light emitting metal halide species periodically "embedded" in a wide band gap organic cationic matrix through ionic bonds. However, achieving efficient blue emissions is challenging for this class of materials, as structural distortions of metal halides often lead to large Stokes shifts. Here we report a highly luminescent blue emitting 0D organic lead bromide, $(C_{13}H_{19}N_4)_2PbBr_4$, with a peak emission of 460 nm (2.70 eV), a full width at half maximum (FWHM) of 66 nm (0.40 eV), a Stokes shift of 111 nm (0.85 eV), and a PLQE of $\sim$ 40%. Single crystal structure analysis shows that individual $PbBr_4^{2-}$ species adopt a near-seesaw structure, which are coordinated to benzyl-hexamethylenetetrammonium $(C_{13}H_{19}N_4^+)$ organic cations. The relatively small Stokes shift as compared to those of previously reported 0D organic metal halide hybrids are attributed to the low chemical reactivity of Pb $6s^2$ long pairs and the rigid organic cationic matrix. $(C_{13}H_{19}N_4)_2PbBr_4$ also shows exceptional stability in air with little-to-no change of properties for more than a year.

Organic-inorganic metal halide hybrids have recently emerged as a class of functional materials that exhibit outstanding performance in various types of optoelectronic devices, such as photovoltaics and light-emitting diodes.[1-6] Zero-dimensional (0D) organic-inorganic metal halide hybrids, defined by the specific crystal structure, in which individual metal halide species are separated from each other by organic cations, have drawn significant research attention, for their extraordinary optical properties.[7-10] Due to the strong spatial confinement of isolated metal halides, the emissions of 0D organic metal halides originate from the radiative decay of localized excitons trapped in individual metal halides, featuring broadband spectra, large Stokes shifts, and high photoluminescence quantum efficiencies (PLQEs).[11-12] These unique and remarkable features make them great candidates as solid-state phosphors, which require minimum self-absorption and high PLQE.

While a large number of 0D organic-inorganic metal halide hybrids have been developed to date, 0D hybrids with efficient blue emissions are still rare.[13-17] Most 0D organic metal halide hybrids have excitation peaks in the near ultraviolet (UV) region, but emit strongly Stokes shifted spectra with peaks of over 500 nm.[4] The primary reason for the large Stokes shifts is that most 0D hybrids have a large degree of structural distortion in the excited state after photoexcitation.[11, 18] To achieve blue emissions, two types of 0D hybrids are potential candidates. Type-I 0D hybrids should have excitation peaks with sufficiently high energy to ensure the coexistence of large Stokes shifts and blue emissions. However, it is not desirable to employ these materials as down conversion phosphors in LEDs, considering the harmful high-energy UV light source required for the photoexcitation and the large energy loss between the excitation and emission. Type-II 0D hybrids, on the other hand, could have near UV excitation if small Stokes shifts could be achieved, which would be more desirable for many applications. Manipulating the degree of Stokes shifts is the key to achieve blue emissions, as well as for color-tuning and energy loss control of 0D organic-inorganic metal halide hybrids.

Here, we report an 0D organic-inorganic hybrid material $(C_{13}H_{19}N_4)_2PbBr_4$, which gives efficient blue emission peaked at 460 nm with a PLQE of 40% upon UV excitation. The optical properties of $(C_{13}H_{19}N_4)_2PbBr_4$ were

characterized by static and time-resolved photoluminescence spectroscopies, showing a very small Stokes shift of 111 nm (0.85 eV) for 0D organic metal halide hybrids. This kind of 0D hybrid with an individual $PbBr_4$ unit as the building block in single crystals had not been reported until very recently during the preparation of this manuscript, when 0D $Bmpip_2PbBr_4$ was reported by Morad *et al*.[14] Compared to $Bmpip_2PbBr_4$, our 0D $(C_{13}H_{19}N_4)_2PbBr_4$ is more centered in the blue part of the spectrum (460 nm vs. 470 nm), and has a much higher PLQE (40% vs. 24%) and smaller Stokes shift (111 nm vs. 123 nm). According to Density Functional Theory (DFT) calculations, we attribute the unusually small Stokes shift to the low chemical reactivity of the Pb $6s^2$ lone pair, resulting in the low extent of structural deformation between the ground state and excited state. Also, the rigid environment of the metal halide anions in the crystal plays an important role in reducing the Stoke-shift of this material.
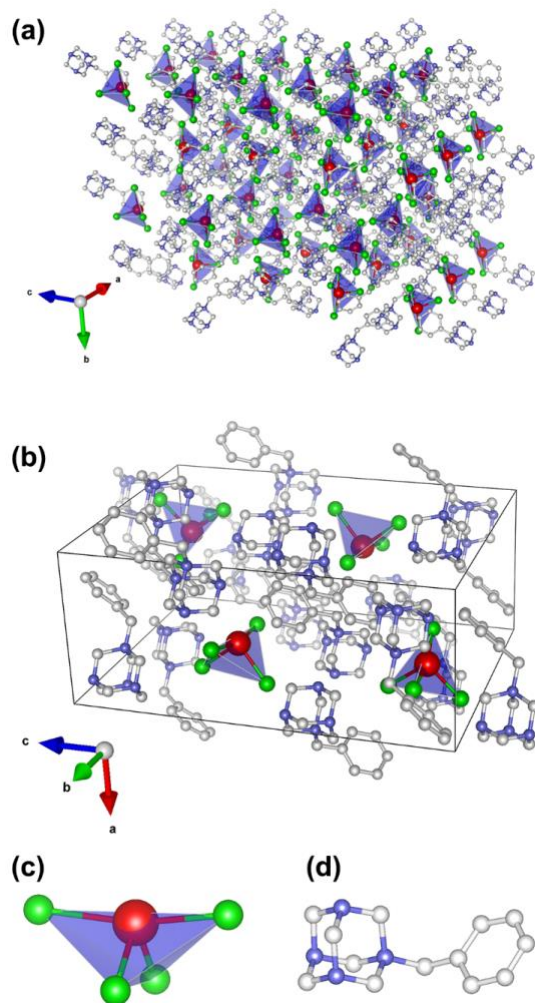

(a)

(b)

(c)   **(d)**

Figure 1. (a) Single crystal structure of $(C_{13}H_{19}N_4)_2PbBr_4$ (red: lead atoms; green: bromine atoms; blue: nitrogen atoms; white: carbon atoms; blue polyhedron: $PbBr_4$ seesaws; hydrogen atoms were hidden for clarity). (b) Monoclinic unit cell of $(C_{13}H_{19}N_4)_2PbBr_4$. (c) Structure of an individual $PbBr_4^{2-}$ seesaw anion. (d) Structure of an individual $C_{13}H_{19}N_4^+$ organic cation.

$(C_{13}H_{19}N_4)_2PbBr_4$ single crystals were synthesized by diffusing dichloromethane into precursor solution of stoichiometrically mixed $C_{13}H_{19}N_4Br$ organic salt and lead bromide. (See Supporting Information for experimental details). Single crystal X-Ray Diffraction (SCXRD) results show that the phase comprises separated $PbBr_4^{2-}$ anions ionically bonded with surrounding bulky organic cations ($C_{13}H_{19}N_4^+$) with a typical 0D organic-inorganic metal halide hybrid structure. (Figure 1a) The single crystal structure exhibits monoclinic $P2_1/c$ symmetry, with all $PbBr_4^{2-}$ units in the same environment and undistinguishable. (Figure 1b) The closest Pb-Pb distance is above 1 nm, ensuring little to no electronic interaction between two seesaw units, which is confirmed by the theoretical calculation below. The $PbBr_4$ near-seesaw structure originates from deformed trigonal bipyramid, with a lone pair on its equatorial plane. (Figure 1c) The bond lengths and angles are listed in Table S1. The stabilization of this near-seesaw structures of $PbBr_4$ is due to the polarizable Pb-6s lone pair.[19] We compared the crystal structure of $(C_{13}H_{19}N_4)_2PbBr_4$ to those of previously reported $(C_9NH_{20})_2SnBr_4$ and $Bmpip_2PbBr_4$. It was found that $(C_{13}H_{19}N_4)_2PbBr_4$ has the most distorted ground state with the smallest axial Br-Pb-Br angle of 160.4°, as compared to the axial Br-Sn-Br angle of 178.8° in $(C_9NH_{20})_2SnBr_4$ and Br-Pb-Br angle of 179.4° in $Bmpip_2PbBr_4$.[14, 20] The powder X-ray diffraction (PXRD) pattern of the ball-milled $(C_{13}H_{19}N_4)_2PbBr_4$ powder is identical to the simulated one based on the SCXRD, confirming the validity of the structure results (Figure S1). It is worth mentioning that $(C_{13}H_{19}N_4)_2PbBr_4$ exhibits excellent ambient stability and that the emission spectrum and PLQE remains unchanged after storage in air in excess of 1 year. Additionally, it is stable under high-intensity UV irradiation (Figure S2) and has a decomposition temperature above 190 ℃ characterized by Thermogravimetry Analysis (TGA) (Figure S3). The first platform is probably caused by breaking of two benzene moieties from the material. The second platform could be loss of other organic components, and the last one related to the decomposition to $PbBr_2$ and complete evaporation.

We then investigated the photophysical properties of $(C_{13}H_{19}N_4)_2PbBr_4$ at both room temperature (r.t.) and 77 K. The $(C_{13}H_{19}N_4)_2PbBr_4$ crystals are colorless under ambient light and exhibit bright blue emission under UV light with a high PLQE of 40%. Static room temperature spectra show that $(C_{13}H_{19}N_4)_2PbBr_4$ excited by UV light with wavelength shorter than 420 nm, has the emission peak at 460 nm, with an FWHM of 66 nm. The corresponding CIE chromaticity coordinates are (0.14, 0.09), very close to the pure blue vertex. (Figure 2c) We also used different excitation wavelengths and found that the emission remains unchanged within a large excitation wavelength window. (Figure S4) A small Stokes shift of 111 nm (0.85 eV) was obtained for this blue emitting material (Figure S5), which, according to the best of our knowledge, is the smallest Stokes shift achieved to date for 0D organic-inorganic metal halide hybrids. The comparison of the optical properties of $(C_{13}H_{19}N_4)_2PbBr_4$, $(C_9NH_{20})_2SnBr_4$ and $Bmpip_2PbBr_4$ is summarized in Table S2. Considering the high color purity and stability, $(C_{13}H_{19}N_4)_2PbBr_4$ may be a good candidate as blue down-converting material to substitute inorganic phosphors containing rare-earth elements. The lifetime of the emission was determined by time-resolved methods (Figure 2b). The average lifetime of the emission at room

temperature is 75 ns based on exponential-fitting (See Supporting Information for detailed calculation). When the temperature was lowered to 77 K, we observed a significant narrowing of the emission peak, with the FWHM lowered from 66 nm (0.40 eV) to 40 nm (0.23 eV). The excitation and emission peaks slightly shifted to 348 nm and 470 nm, respectively, and the PL lifetime increases to 16.4 μs, as determined by single-exponential-fitting of the decay curve. It is worth noting that the emission remains excitation independent at 77 K (Figure S6), indicating that the PL mechanism remains likely the same in the temperature range from 77 K to room temperature. The Stokes shifted emission and relatively long emission lifetime are the characteristics of the 0D organic-inorganic metal halide hybrids, which suggest the PL is the result of the radiative decay of localized excitons on the isolated metal halides, supported by the theoretical calculations below.
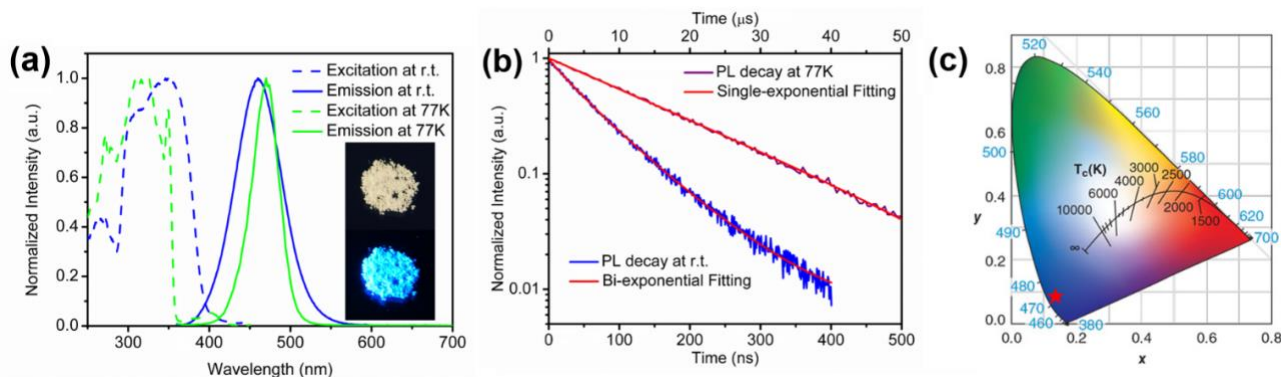

Figure 2. (a) Excitation (blue dash line probed at 460 nm at room temperature, green dash line probed at 470 nm at 77 K) and emission spectra (blue line excited by 360 nm light at room temperature, green line excited by 350 nm light at 77 K) of $(C_{13}H_{19}N_4)_2PbBr_4$ crystals. Inset: photoimage of $(C_{13}H_{19}N_4)_2PbBr_4$ crystals under ambient light (top) and under UV irradiation (bottom). (b) Time-resolved PL decay of the maximum PL peaks and fitting of the decay curves at room temperature (probed at 460 nm, blue line, x axial at the bottom) and 77 K (probed at 470 nm, violet line, x axial at the top) (c) Commission Internationale de l'Eclairage (CIE) chromaticity coordinates of the emission from $(C_{13}H_{19}N_4)_2PbBr_4$ (red star).

To elucidate the origin of the small Stokes shift of $(C_{13}H_{19}N_4)_2PbBr_4$, we firstly conducted the calculation based on DFT. The calculated band structure of $(C_{13}H_{19}N_4)_2PbBr_4$ (Figure 3a) exhibits flat bands, indicating that the electronic states are highly localized, consistent with its 0D crystal structure and no Pb-Pb interactions. The valence band maximum (VBM) (at the M point) and the conduction band minimum (CBM) (between Γ and Z points) are both derived from the electronic states confined within the $(PbBr_4)^{2-}$ metal halide units as evidenced by the calculated DOS in Figure 3b; the former is primarily made up of Br-4p and Pb-6s orbitals while the latter has a mixed Pb-6p and Br-4p character. The band gap is slightly indirect. The PBE band gap at the Γ point is 3.17 eV, which is expected to be underestimated due to the well know PBE band gap error, and the hybrid PBE0 calculation increases the band gap at the Γ point to 4.89 eV. The partial DOS on the $C_{13}H_{19}N_4^+$ molecule near the band gap is derived from the π orbitals on the phenyl rings. However, a close examination of the VBM and CBM found little contribution from organic cations. The axial and the equatorial Pb-Br bond lengths in the near-seesaw structure of $PbBr_4$ were calculated to be 3.00 Å and 2.77 Å respectively, and the Br-Pb-Br bond angle between the two axial Pb-Br bonds and that between the two equatorial Pb-Br bonds were calculated to be 160.42° and 94.08° respectively. These calculated bond lengths and angles are in excellent agreement with the corresponding experimental values: 2.99 Å, 2.74 Å, 164.15°, and 93.57°. (Table S1)
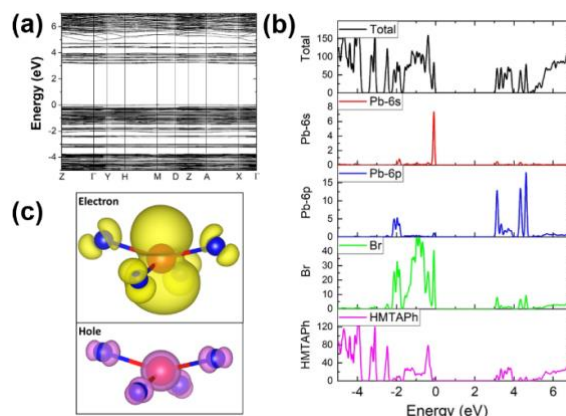

Figure 3. (a) Electronic band structure of $(C_{13}H_{19}N_4)_2PbBr_4$ calculated using the PBE functional. Note that the band gap is underestimated. (b) Density of states (DOS) of $(C_{13}H_{19}N_4)_2PbBr_4$ calculated using the PBE functional. (The $C_{13}H_{19}N_4$ is simplified as HMTAPh) Note that the band gap is underestimated. (c) The partial densities of the electron and hole in the exciton. The Pb and the Br atoms are represented by red and blue balls, respectively.

The excitation of an electron-hole pair results in an exciton localized on a single $PbBr_4$, which, in turn, dynamically distorts its structure. The excited hole state is a σ-like anti-bonding state between Pb-6s and Br-4p centered at the Pb ion and the excited electron state is a π-like anti-bonding orbital between Pb-6p and Br-4p (Figure 3c). The Coulomb repulsion from the excited electron in the

Pb-6p dangling bond flattens the structure and the excited state of PbBr$_4$ is closer to a tetrahedron. The length of axial Pb-Br bonds is shortened from 2.99 Å to 2.90 Å due to the increased Coulomb attraction while that of the equatorial Pb-Br bonds is increased slightly from 2.77 Å to 2.78 Å. The axial and equatorial Br-Pb-Br bond angles in the excited state are similar, 149.40° and 146.29°, respectively. When compared with the reported (C$_9$NH$_{20}$)$_2$SnBr$_4$, the degree of excited-state structural distortion in (C$_{13}$H$_{19}$N$_4$)$_2$PbBr$_4$ is much reduced, as shown by the smaller axial and equatorial bond angles change in Table S1, which was attributed to the chemically more stable Pb-6s lone pair than Sn-5s lone pair.[19] As a result, the calculated exciton relaxation energy and the Stokes shift in (C$_{13}$H$_{19}$N$_4$)$_2$PbBr$_4$ (0.41 eV and 1.15 eV) are significantly lower than those in (C$_9$NH$_{20}$)$_2$SnBr$_4$ (1.42 eV and 2.46 eV). Both the Pb and Sn ions in their respective Pb and Sn halides are four-fold coordinated in a seesaw structure. Therefore, the stereochemical activity is not the driving force behind the difference in the ground- and excited states of the Pb and Sn halides. The calculated exciton excitation and emission energies of (C$_{13}$H$_{19}$N$_4$)$_2$PbBr$_4$ and (C$_9$NH$_{20}$)$_2$SnBr$_4$ agree well with the experimental values (Table S2) proving the reliability of the calculation method.
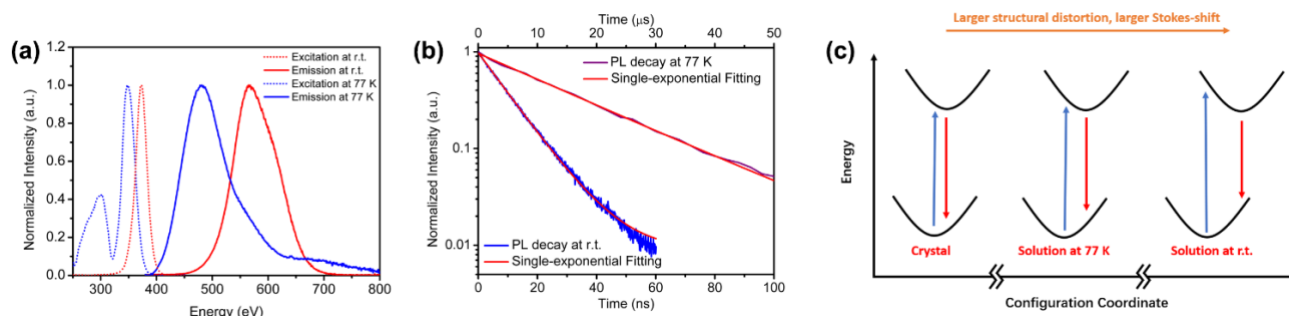

Figure 4. (a) Excitation (red dash line probed at 566 nm at room temperature, blue dash line probed at 480 nm at 77 K) and emission spectra (red line excited by 360 nm light at room temperature, green line excited by 360 nm light at 77 K) of (C$_{13}$H$_{19}$N$_4$)$_2$PbBr$_4$ precursor solution (0.027 M) in dimethylformamide. (b) Time-resolved PL decay and fitting of the decay curves at room temperature (probed at 566 nm, blue line, x axial at the bottom) and 77 K (probed at 480 nm, violet line, x axial at the top). (c) Energy diagram showing the ground states and excited states of crystal at 77 K, solution at 77 K and solution at r.t.

Other than the contribution of the stable 6s^2 lone pair, the rigidity of the organic C$_{13}$H$_{19}$N$_4^+$ cations also plays an important role in lowering the Stokes shift of (C$_{13}$H$_{19}$N$_4$)$_2$PbBr$_4$. Since C$_{13}$H$_{19}$N$_4^+$ is rigid in the solid state when compared with other more flexible organic cations with alkyl chains, it is reasonable to assume that PbBr$_4$ seesaws are in a more confined environment in this particular crystal lattice, which hinders structural reorganization upon excitation. To prove this, we have further characterized the optical spectra of (C$_{13}$H$_{19}$N$_4$)$_2$PbBr$_4$ in solution at room temperature and a frozen solution at 77 K. (Figure 4a, preparation of the solution in Supporting Information) According to previous studies, we assume that the main emissive species in the solution are PbBr$_4^{2-}$ anions.[21] The lifetime of the precursor solution at r.t and at 77 K are 10.3 ns and 16.1 μs, respectively. (Figure 4b, lifetime calculation in Supporting Information) The PL emission spectra of the solution at 77 K and its lifetime are similar to those of the single crystals at 77 K, indicating the above assumption is practical. Interestingly, we found a trend of blue shifting of both excitation peak and emission peak from solution to frozen solution to solid state. On the other hand, the Stokes shift is also reduced from 1.14 eV for solution at r.t. to 0.92 eV for single crystals at 77 K following the trend. The reason is that in dilute solution at room temperature, PbBr$_4^{2-}$ ions are surrounded by solvent molecules which have weak interactions with the anions and thus small spatial confinement effects. When the solution is frozen, the solvent molecules could barely move resulting in a more rigid environment for PbBr$_4$. For the single crystals at 77K, the PbBr$_4^{2-}$ anions are surrounded by C$_{13}$H$_{19}$N$_4^+$ organic cations, which are bulkier, more rigid, and ionically bonded. As a result, PbBr$_4$ anions in crystals have the furthermost spatial confined environment and should undergo the least extent of structural deformation upon excitation among the three. The energy diagram is drawn in Figure 4c to show the difference. This is further evidenced by comparing the structures of the cations in (C$_{13}$H$_{19}$N$_4$)$_2$PbBr$_4$ and Bmpip$_2$PbBr$_4$.[14] Bmpip contains more alkyl chains and thus is more flexible than C$_{13}$H$_{19}$N$_4^+$, which may provide a less confined environment for PbBr$_4$ ions. As a result, the Stokes shift for Bmpip$_2$PbBr$_4$ was determined to be 0.9 eV which is slightly larger than the 0.85 eV Stokes shift for (C$_{13}$H$_{19}$N$_4$)$_2$PbBr$_4$ at room temperature. All these data suggest that more rigid organic cations benefit the formation of 0D hybrid materials with smaller Stokes shift.

In conclusion, a new blue emitting (emission peaked at 460 nm) organic-inorganic metal halide hybrid (C$_{13}$H$_{19}$N$_4$)$_2$PbBr$_4$ with high PLQE of ~ 40 % was developed. The lead bromides anion adopts a rare near-seesaw structure in the 0D crystal lattice resulting from the polarization of the Pb 6s^2 lone pair. The optical behavior of (C$_{13}$H$_{19}$N$_4$)$_2$PbBr$_4$ indicates the blue emission is from localized excitons residing on the metal halides. According to theoretical calculation and reduced Stokes shift from from solution to solid state crystals, we attribute the unusually small Stokes-shift of the material to the low chemical reactivity of the Pb 6s^2 lone pair electrons and the

spatial confinement effect introduced by the rigid organic cations. This work not only illustrates a new efficient blue light emitter but also suggests a new method to manipulate the optical properties of 0D organic-inorganic metal halide hybrids.

ASSOCIATED CONTENT

Supporting Information.
The Supporting Information is available free of charge via the Internet at http://pubs.acs.org.
Experimental procedures, PXRD, photostability, TGA, excitation and emission data of $(C_{13}H_{19}N_4)_2PbBr_4$ (docx)
Crystallographic information file of $(C_{13}H_{19}N_4)_2PbBr_4$ (CIF)

AUTHOR INFORMATION

Corresponding Author

* E-mail: bma@fsu.edu

Notes
Any additional relevant notes should be placed here.

ACKNOWLEDGMENT

REFERENCES

(1) Yang, W. S.; Park, B. W.; Jung, E. H.; Jeon, N. J.; Kim, Y. C.; Lee, D. U.; Shin, S. S.; Seo, J.; Kim, E. K.; Noh, J. H.; Seok, S. I. Iodide management in formamidinium-lead-halide-based perovskite layers for efficient solar cells. *Science* **2017**, *356*, 1376-1379.

(2) Ng, C. H.; Lim, H. N.; Hayase, S.; Zainal, Z.; Huang, N. M. Photovoltaic performances of mono- and mixed-halide structures for perovskite solar cell: A review. *Renew. Sust. Energ. Rev.* **2018**, *90*, 248-274.

(3) Chen, P.; Bai, Y.; Lyu, M. Q.; Yun, J. H.; Hao, M. M.; Wang, L. Z. Progress and Perspective in Low-Dimensional Metal Halide Perovskites for Optoelectronic Applications. *Sol. RRL* **2018**, *2*, 1700186.

(4) Zhou, C.; Lin, H.; He, Q.; Xu, L.; Worku, M.; Chaaban, M.; Lee, S.; Shi, X.; Du, M.-H.; Ma, B. Low dimensional metal halide perovskites and hybrids. *Mater. Sci. Eng., R* **2019**, *137*, 38-65.

(5) Zhao, B.; Bai, S.; Kim, V.; Lamboll, R.; Shivanna, R.; Auras, F.; Richter, J. M.; Yang, L.; Dai, L.; Alsari, M.; She, X.-J.; Liang, L.; Zhang, J.; Lilliu, S.; Gao, P.; Snaith, H. J.; Wang, J.; Greenham, N. C.; Friend, R. H.; Di, D. High-efficiency perovskite–polymer bulk heterostructure light-emitting diodes. *Nat. Photonics* **2018**, *12*, 783-789.

(6) Zhang, H.; Liao, Q.; Wu, Y.; Zhang, Z.; Gao, Q.; Liu, P.; Li, M.; Yao, J.; Fu, H. 2D Ruddlesden-Popper Perovskites Microring Laser Array. *Adv. Mater.* **2018**, *30*, e1706186.

(7) Wang, Z. P.; Wang, J. Y.; Li, J. R.; Feng, M. L.; Zou, G. D.; Huang, X. Y. [Bmim]2SbCl5: a main group metal-containing ionic liquid exhibiting tunable photoluminescence and white-light emission. *Chem. Commun.* **2015**, *51*, 3094-3097.

(8) Xu, L. J.; Sun, C. Z.; Xiao, H.; Wu, Y.; Chen, Z. N. Green-Light-Emitting Diodes based on Tetrabromide Manganese(II) Complex through Solution Process. *Adv. Mater.* **2017**, *29*, 1605739.

(9) Zhou, C. K.; Lin, H. R.; Tian, Y.; Yuan, Z.; Clark, R.; Chen, B. H.; van de Burgt, L. J.; Wang, J. C.; Zhou, Y.; Hanson, K.; Meisner, Q. J.; Neu, J.; Besara, T.; Siegrist, T.; Lambers, E.; Djurovich, P.; Ma, B. W. Luminescent zero-dimensional organic metal halide hybrids with near-unity quantum efficiency. *Chem. Sci.* **2018**, *9*, 586-593.

(10) Zhou, J.; Li, M.; Ning, L.; Zhang, R.; Molokeev, M. S.; Zhao, J.; Yang, S.; Han, K.; Xia, Z. Broad-Band Emission in a Zero-Dimensional Hybrid Organic [PbBr6] Trimer with Intrinsic Vacancies. *J. Phys. Chem. Lett.* **2019**, *10*, 1337-1341.

(11) Han, D.; Shi, H. L.; Ming, W. M.; Zhou, C. K.; Ma, B. W.; Saparov, B.; Ma, Y. Z.; Chen, S. Y.; Du, M. H. Unraveling luminescence mechanisms in zero-dimensional halide perovskites. *J. Mater. Chem. C* **2018**, *6*, 6398-6405.

(12) Cortecchia, D.; Yin, J.; Petrozza, A.; Soci, C. White light emission in low-dimensional perovskites. *J. Mater. Chem. C* **2019**, *7*, 4956-4969.

(13) Zhou, C.; Lin, H.; Worku, M.; Neu, J.; Zhou, Y.; Tian, Y.; Lee, S.; Djurovich, P.; Siegrist, T.; Ma, B. Blue Emitting Single Crystalline Assembly of Metal Halide Clusters. *J. Am. Chem. Soc.* **2018**, *140*, 13181-13184.

(14) Morad, V.; Shynkarenko, Y.; Yakunin, S.; Brumberg, A.; Schaller, R. D.; Kovalenko, M. V. Disphenoidal Zero-Dimensional Lead, Tin, and Germanium Halides: Highly Emissive Singlet and Triplet Self-Trapped Excitons and X-ray Scintillation. *J. Am. Chem. Soc.* **2019**, *141*, 9764-9768.

(15) Lin, J.; Chen, H.; Kang, J.; Quan, L. N.; Lin, Z.; Kong, Q.; Lai, M.; Yu, S.; Wang, L.; Wang, L.-w.; Toney, M. F.; Yang, P. Copper(I)-Based Highly Emissive All-Inorganic Rare-Earth Halide Clusters. *Matter* **2019**, *1*, 180-191.

(16) Jun, T.; Sim, K.; Iimura, S.; Sasase, M.; Kamioka, H.; Kim, J.; Hosono, H. Lead-Free Highly Efficient Blue-Emitting Cs3 Cu2 I5 with 0D Electronic Structure. *Adv. Mater.* **2018**, *30*, e1804547.

(17) Roccanova, R.; Yangui, A.; Nhalil, H.; Shi, H.; Du, M.-H.; Saparov, B. Near-Unity Photoluminescence Quantum Yield in Blue-Emitting $Cs_3Cu_2Br_{5-x}I_x$ (0 ≤ x ≤ 5). *ACS Appl. Electron. Mater.* **2019**, *1*, 269-274.

(18) Cortecchia, D.; Yin, J.; Bruno, A.; Lo, S. Z. A.; Gurzadyan, G. G.; Mhaisalkar, S.; Bredas, J. L.; Soci, C. Polaron self-localization in white-light emitting hybrid perovskites. *J. Mater. Chem. C* **2017**, *5*, 2771-2780.

(19) Shi, H.; Han, D.; Chen, S.; Du, M.-H. Impact of metal ns2 lone pair on luminescence quantum efficiency in low-dimensional halide perovskites. *Phys. Rev. Mater.* **2019**, *3*, 034604.

(20) Zhou, C.; Lin, H.; Shi, H.; Tian, Y.; Pak, C.; Shatruk, M.; Zhou, Y.; Djurovich, P.; Du, M. H.; Ma, B. A Zero-Dimensional Organic Seesaw-Shaped Tin Bromide with Highly Efficient Strongly Stokes-Shifted Deep-Red Emission. *Angew. Chem. Int. Ed.* **2018**, *57*, 1021-1024.

(21) Oldenburg, K.; Vogler, A. Electronic Spectra and Photochemistry of Tin(II), Lead(II), Antimony(III), and Bismuth(III) Bromide Complexes in Solution. *Z. Naturforsch. B* **1993**, *48*, 1519.